Large-N analysis of the critical behavior of the topological Ginzburg-Landau theory of self-dual Josephson junction arrays

S. Sakhi*

College of Arts and Sciences, American University of Sharjah,
P.O. Box 26666, Sharjah, United Arab Emirates

(Received 18 June 2014; published 21 August 2014)

Using large-N technique at fixed dimension ($d = 3$), I examine the multicritical behavior of a $U(N/2) \times U(N/2)$ Ginzburg-Landau theory of two multicomponent complex fields interacting through gauge fields described by Maxwell terms and a mixed Chern-Simons term. This model is relevant to the dynamics of Cooper pairs and vortices in a self-dual Josephson junction array system near its superconductor-insulator quantum transition. I present calculations of the various critical exponents including $1/N$ corrections to the $N = \infty$ saddle point. I investigate in the scaling region the behavior of the renormalized zero-momentum four-point quartic couplings u and w in the action, and I calculate the $1/N$ correction to the β-functions and their fixed-point values. It is shown that the decoupled fixed point is destabilized in the presence of the mixed Chern-Simons term at the next-to-leading order. Finally, I examine the universal character of the conductivity at the critical point up to the next-to-leading order in $1/N$ expansion.

DOI: 10.1103/PhysRevD.90.045028 PACS numbers: 11.10.Kk, 11.15.Pg, 74.20.De, 74.81.Fa

I. INTRODUCTION

The continuous quantum phase transition (QPT) [1] in Josephson junction arrays systems (JJA) provides an ideal example to study quantum fluctuations at zero temperature. Near a quantum critical point [2], scale invariance and universality emerge, and the long-distance low energy properties of the system are characterized by critical exponents that are insensitive to the microscopic details of the model [2]. A topological two-field Ginzburg-Landau theory interacting through gauge fields was introduced in [3] as a phenomenological model to study the QPT in JJA systems. Via a duality transformation, the currents of Cooper pairs (p_μ) and vortices (ℓ_μ) in the underlying microscopic model are represented as the dual field strength of fictitious gauge fields $p_\mu = \epsilon^{\mu\nu\lambda}\partial_\nu b_\lambda$ and $\ell_\mu = \epsilon^{\mu\nu\lambda}\partial_\nu a_\lambda$, with $\epsilon_{\mu\nu\lambda}$ ($\mu, \nu, \lambda = 0, 1, 2$) being the antisymmetric Levi-Civita symbol [4]. When written in terms of the gauge fields, these currents are trivially conserved due to the presence of the $\epsilon_{\mu\nu\lambda}$ symbol. In the dual description, kinetic terms for charges and vortices are expressed by Maxwell terms for a_μ and b_μ, while the Lorentz force exerted by the vortices on the charges and the Magnus force exerted by the charges on the vortices are expressed by a mixed Chern-Simons term $\epsilon^{\mu\nu\lambda}a_\mu\partial_\nu b_\lambda$ [4]. Along with emerging gauge fields, two complex scalar fields are introduced to account for quantum disorder due to electric and magnetic excitations in the system. The resulting low energy effective model is a Ginzburg-Landau theory with two disorder fields coupled to a Maxwell-mixed-Chern-Simons gauge theory [3].

The competition between the disordering fields exhibits multicritical point behavior. This was investigated in a recent paper [3] where a rich phase diagram was found. The renormalization group (RG) analysis was done at fixed dimension $D = 3$ and not in $D = 4 - \epsilon$ as is often done because of the presence of the Chern-Simons term, which is an intrinsically three-dimensional object. This fixed-dimension approach to critical phenomena was introduced by Parisi in his study of a pure $u\phi^4$ theory [5]. It draws on the fact that near the critical point the system has only one relevant length scale, the correlation length, which diverges at this point. This length is used to convert dimensionful coupling constants into dimensionless ones. The dimensionless bare coupling $g_0 = u/m$ used in the expansion diverges when the mass m goes to zero, resulting in a useless perturbative expansion near the transition. To find a more suitable expansion parameter other than the bare coupling, one introduces a field renormalization and a renormalized dimensionless coupling constant g as in four dimensions, and one looks for an infrared (IR) stable zero in the corresponding Callan-Symanzik $\beta(g)$—function. It ensues that the renormalized coupling has a finite limit g_c when the bare coupling becomes large. In contrast with the ϵ-expansion, however, at fixed dimension no small parameter is available to control the calculation. In the absence of a parameter other than the nonlinearity g to systematically control the computation, accurate determinations of the fixed-point (FP) value of the coupling and all other physical quantities hinge on the analytic properties of the series, in addition to the number of terms available [6]. This limitation of the approximate one-loop renormalization group at fixed dimension prompts us to look for another method to solve our model beyond perturbation

*ssakhi@aus.edu

theory and obtain confirmation of the perturbative results found in [3].

In this paper I concentrate on the critical behavior of the $d = 2 + 1$ dimensional $U(N/2) \times U(N/2)$ Ginzburg-Landau-mixed-Chern-Simons theory in the framework of the $1/N$ expansion. Large-N expansion has many applications in quantum field theory and statistical mechanics. Since this method applies to any dimension of space, it was particularly useful in revealing some of the most fundamental aspects of critical phenomena. The study of spin systems in the large-N limit began with the work of Stanley [7], who studied the N vector model using the saddle point technique. Its application to critical phenomena was carried out by Ma [8], who calculated $1/N$ corrections to the critical exponents and explained in the same context the Wilson renormalization group ideas. Calculations in continuum field theory were performed in [9] and nonlinear sigma models [10]. The advantage of such a technique is that $1/N$ provides a new expansion parameter that allows the summation of infinite classes of Feynman graphs and the results have a nonperturbative interpretation. It turns out that this model is renormalizable in the $1/N$ expansion, and its critical exponents can be obtained in a systematic way. The critical exponents ν, η, and γ are calculated to the $O(1/N)$. Next we study the renormalized zero-momentum four-point couplings of the model by applying the $1/N$ expansion. We compute the next-to-leading $1/N$ correction to the renormalized couplings as a function of the bare couplings and the renormalized mass. From these we find the $1/N$ correction to the β-functions and the fixed-point values. Finally, I examine the universal character of the conductivity at the critical point up to the next-to-leading order in $1/N$ expansion.

II. THE CONTINUUM MODEL

The low energy effective field theory describing the dynamics of Cooper pairs and vortices in a self-dual Josephson junction array consists of two complex fields associated with disordering due to electric charges (Ψ) and magnetic charges (Φ) interacting through fictitious gauge fields a_μ and b_μ. The derivation has been presented before [3], and the Euclidean Lagrangian is given by

$$L = L_S + U + L_G, \tag{1}$$

$$L_S = |(\partial_\mu - ia_\mu)\Psi|^2 + |(\partial_\mu - ib_\mu)\Phi|^2$$
$$U = r(|\Psi|^2 + |\Phi|^2) + \frac{u_0}{2}(|\Psi|^4 + |\Phi|^4) + w_0|\Psi|^2|\Phi|^2, \tag{2}$$

$$L_G = \frac{1}{4e_b^2} f_{\mu\nu}^2 + \frac{1}{4e_a^2} g_{\mu\nu}^2 + i\kappa b_\mu \epsilon^{\mu\nu\lambda}\partial_\nu a_{\lambda.} \tag{3}$$

Because of quantum fluctuations and RG iterations, we start with the most general Landau-Ginzburg-Wilson Lagrangian that is symmetric under $U(1) \times U(1)$ transformations and contains up to quartic interaction terms described by couplings u and w between Φ and Ψ fields. The first two terms in L_G are the usual Maxwell terms for the gauge fields b_μ, a_μ, associated with the currents of Cooper pairs and vortices in the JJA system. Notice that we have two different gauge couplings, which are related to the parameters of the JJA system: $e_a^2 = 8E_C$ and $e_b^2 = 4\pi^2 E_J$ where E_J, the Josephson coupling energy, measures the strength for the phase coupling between two superconducting islands and E_C, the charging energy required to add extra charges to neutral islands. The mixed Chern-Simons term has a coefficient $\kappa = 1/\pi$ [3].

III. ONE-LOOP RENORMALIZATION GROUP ANALYSIS IN THREE DIMENSIONS

Before we construct the $1/N$ expansion of the massive scaling regime, it is instructive to summarize some properties of this field theory from the point of view of perturbative RG in the same regime. This way one will be able to compare large-N results with RG predictions. We note that the construction of the perturbative renormalization expansion in the massless regime of model (1) was recently reported in [3]. At one-loop and for $N/2$-component complex scalar fields, one introduces renormalized Ψ_R, Φ_R, $a_{\mu,R}$, and $b_{\mu,R}$ fields, which are proportional to the bare ones:

$$\Psi_R = Z_\Psi^{-1/2}\Psi, \qquad \Phi_R = Z_\Phi^{-1/2}\Phi, \qquad a_{\mu,R} = Z_a^{-1/2}a_\mu,$$
$$b_{\mu,R} = Z_b^{-1/2}b_\mu. \tag{4}$$

The constants of proportionality are fixed by imposing normalization conditions on the one-particle irreducible two-point $\Gamma^{(2)R}(k)$ and four-point $\Gamma^{(4)R}(0,0,0,0)$ functions

$$\Gamma^{(2)R}(k=0) = m^2, \qquad \left.\frac{\partial\Gamma^{(2)R}(k)}{\partial k^2}\right|_{k^2=0} = 1, \tag{5}$$

$$\Gamma_{1,1}^{(4)R}(0,0,0,0) = \Gamma_{2,2}^{(4)R}(0,0,0,0) = 3m\hat{u}_R, \tag{6}$$

$$\Gamma_{1,2}^{(4)R}(0,0,0,0) = m\hat{w}_R, \tag{7}$$

$$\frac{1}{2}\frac{\partial}{\partial k^2}[P_T^{\mu\nu}(k)\Gamma_{a,\nu\mu}^{(2)R}(k)]_{k=0} = \frac{1}{m\hat{e}_{a,R}^2}, \tag{8}$$

$$\frac{1}{2}\frac{\partial}{\partial k^2}[P_T^{\mu\nu}(k)\Gamma_{b,\nu\mu}^{(2)R}(k)]_{k=0} = \frac{1}{m\hat{e}_{b,R}^2}, \tag{9}$$

where the mass m was used to define the renormalized dimensionless coupling constants with hats and $P_T^{\mu\nu}(k)$ is the transverse projection given by $P_T^{\mu\nu}(k) = \delta^{\mu\nu} - k^\mu k^\nu/k^2$. Up to one-loop order, the relevant Feynman diagrams for the four-point $\Gamma_{1,1}^{(4)}$ and $\Gamma_{1,2}^{(4)}$ functions at zero external momenta are shown in Fig. 1. These lead to the flow equations in three space-time dimensions:

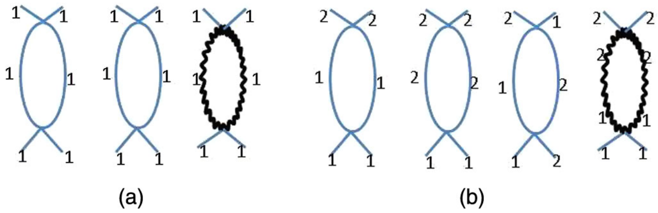

FIG. 1 (color online). (a) $\Gamma_{11}^{(4)}$ and (b) $\Gamma_{12}^{(4)}$ to one loop. The solid lines represent the scalar field propagators with 1 corresponding to Ψ and 2 to Φ. The wiggly lines represent the gauge propagators with 1 corresponding to a_μ and 2 to b_μ.

$$\beta(\hat{u}_R) = \frac{d\hat{u}_R}{d\ln(m)} = (2\eta_\Psi - 1)\hat{u}_R + \frac{N+8}{16\pi}\hat{u}_R^2 + \frac{N}{16\pi}\hat{w}_R^2, \quad (10)$$

$$\beta(\hat{w}_R) = \frac{d\hat{w}_R}{d\ln(m)} = (\eta_\Phi + \eta_\Psi - 1)\hat{w}_R + \frac{N+2}{8\pi}\hat{u}_R\hat{w}_R + \frac{\hat{w}_R^2}{4\pi}, \quad (11)$$

$$\beta(\hat{e}_{a,R}^2) = \frac{d\hat{e}_a^2}{d\ln(m)} = -\hat{e}_{a,R}^2\left(1 - \frac{N}{48\pi}\hat{e}_{a,R}^2\right), \quad (12)$$

$$\beta(\hat{e}_{b,R}^2) = \frac{d\hat{e}_b^2}{d\ln(m)} = -\hat{e}_{b,R}^2\left(1 - \frac{N}{48\pi}\hat{e}_{b,R}^2\right), \quad (13)$$

where the η-exponents, which characterize the anomalous dimensions of the two-point correlation functions, are given by

$$\eta_\Phi = -\frac{2}{3\pi}\frac{\hat{e}_{a,R}^2}{(\hat{M}+1)^2}, \qquad \eta_\Psi = -\frac{2}{3\pi}\frac{\hat{e}_{b,R}^2}{(\hat{M}+1)^2}, \quad (14)$$

with $\hat{M} = \kappa\hat{e}_{a,R}\hat{e}_{b,R}$. Note that the beta functions for the gauge charges can also be given exactly in terms of the anomalous dimensions of the gauge fields by $\beta(\hat{e}_{a,R}^2) = \hat{e}_{a,R}^2(\eta_a - 1)$ and $\beta(\hat{e}_{b,R}^2) = \hat{e}_{b,R}^2(\eta_b - 1)$, where $\eta_a = d\ln(Z_a)/d\ln(m)$ and $\eta_a = d\ln(Z_a)/d\ln(m)$. In this form, the existence of a charged fixed point, $\hat{e}_{a,R}^2 \neq 0, \hat{e}_{b,R}^2 \neq 0$, has the immediate consequence that $\eta_a = 1$, $\eta_b = 1$ [11]. The beta functions associated with the gauge couplings have nontrivial solutions when $\hat{e}_a^2 = 48\pi/N$ and $\hat{e}_b^2 = 48\pi/N$. These lead to the fully charged FPs with respect to both gauge fields. There exist four fixed points: (1) Gaussian, at $\hat{u}=\hat{w}=0$, (2) $U(N)$ symmetric, at $\hat{u}=\hat{w}=8\pi(1-2\eta)/(N+4)$, (3) decoupled fixed point, at $\hat{u} = 16\pi(1-2\eta)/(N+8)$ and $\hat{w} = 0$, and (4) mixed, at $\hat{u} = 8\pi(1-2\eta)/(N^2+8)$ and $\hat{w} = 8\pi(1-2\eta)(4-N)/(N^2+8)$. The flows of the interaction coupling constants for different numbers of component N in the critical planes $\hat{e}_a^2 = \hat{e}_b^2 = 48\pi/N$ are depicted in Fig. 2. The infrared stability of these

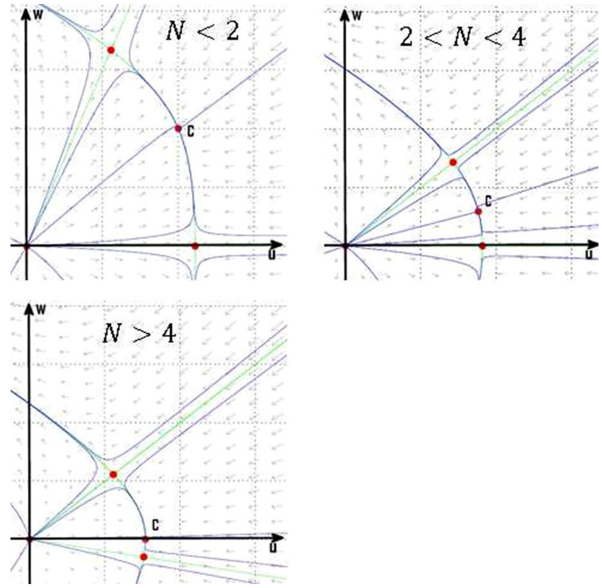

FIG. 2 (color online). One-loop renormalization group flows in the $(\hat{u}, \hat{w})$ plane at fixed dimension $d = 3$.

fixed points is done as usual through the positivity analysis of the eigenvalues of the matrix $M_{ij} = \frac{\partial\beta(\lambda_i)}{\partial\lambda j}$, $\lambda_i = (\hat{u}, \hat{w}, \hat{e}_a^2, \hat{e}_b^2)$, at each fixed point. The result of such study shows that for $N < 2$, the stable fixed point is the one with the enlarged $U(N)$ symmetry. For $2 < N < 4$, on the other hand, the mixed fixed point becomes the stable one. Finally, for $N > 4$ the decoupled fixed point is stable.

IV. LARGE-N EXPANSION

The calculation proceeds in standard fashion, making the assumption that u and w are both of order $1/N$. The complex scalar fields have both $N/2$ components. The solution of the model in the large-N limit is inspired by the central limit theorem [12]. It can be expected that, for N large, $O(N)$ invariant quantities like $|\Phi|^2$ self-average and therefore have small fluctuations. This suggests taking $|\Phi|^2$ and $|\Psi|^2$ as dynamical variables, rather than Φ and Ψ. To implement this idea, one introduces auxiliary fields λ_α and ρ_α and imposes the constraint $\rho_1(x) = |\Psi|^2/N$ and $\rho_2(x) = |\Phi|^2/N$ by integrals over λ_1 and λ_2. The new representation of the partition function is

$$Z = \int d\Psi d\Phi[d\lambda_i d\rho_j]da_\mu db_\mu \exp[-S]$$

$$S = \int_x \left[L_S + i\lambda_1(|\Psi|^2 - N\rho_1) + i\lambda_2(|\Phi|^2 - N\rho_2) + NU + \frac{N}{2}L_G\right], \quad (15)$$

where the integration is over $(2+1)$-dimensional space and imaginary time and $U(\rho_1,\rho_2) = r(\rho_1+\rho_2) + u(\rho_1^2+\rho_2^2)/2 + w\rho_1\rho_2$. The field integral is then Gaussian in Φ and Ψ and can be performed making the dependence of the partition function on N more explicit:

$$Z = \int [d\lambda_i d\rho_j] da_\mu db_\mu \times \exp\left[-\int_x \left(\frac{N}{2}L_G + NU + N(\lambda_1\rho_1 + \lambda_2\rho_2)\right)\right] \times \exp -\frac{N}{2}[\mathrm{tr}\ \ln((i\partial_\mu + a_\mu)^2 - i\lambda_1) + \mathrm{tr}\ \ln((i\partial_\mu + b_\mu)^2 - i\lambda_2)]. \quad (16)$$

The integration over each component of Φ and Ψ has generated the determinant of a differential operator, which is not a simple quantity since λ_1, λ_2, a_μ, and b_μ are fluctuating fields. Fortunately, the calculations that follow require only a perturbative definition valid when λ_1 and λ_2 fluctuate only weakly around some constant imaginary value. Furthermore, since the potential U is quadratic the integral over ρ_1 and ρ_2 is Gaussian and can thus be calculated explicitly. One finds

$$Z = \int [d\lambda_i] da_\mu db_\mu \exp[-S_{\mathrm{eff}}]$$

$$S_{\mathrm{eff}} = \frac{N}{2}\int_x [L_G + (\gamma^+ + \gamma^-)(\lambda_1^2 + \lambda_2^2)/2 + (\gamma^+ - \gamma^-)\lambda_1\lambda_2 - 2ir\gamma^+(\lambda_1 + \lambda_2)] + \frac{N}{2}[\mathrm{tr}\ \ln((i\partial_\mu + a_\mu)^2 - i\lambda_1) + \mathrm{tr}\ \ln((i\partial_\mu + b_\mu)^2 - i\lambda_2)], \quad (17)$$

where $\gamma^\pm = 1/(u_0 \pm w_0)$. In the large-N limit, S_{eff} is of order N and the integral can thus be evaluated by the steepest descent method. We look for a uniform saddle point $\lambda_\alpha = im^2$, $\alpha = 1, 2$ with $m > 0$. Differentiating S_{eff} with respect to λ_α, we find saddle point equation

$$r = m^2 - \frac{1}{2\gamma^+}\int_k \frac{1}{k^2 + m^2}, \quad (18)$$

where we now adopt the convention that the Fourier transform integral $\int_k \equiv \int d^3k/(2\pi)^3$, which we will use throughout this paper. At $N = \infty$ the system becomes critical when $m = 0$, i.e., at $r = r_c$. The saddle point equation becomes

$$\tau = m^2 + \frac{m}{8\pi\gamma^+}, \quad (19)$$

where $\tau = r - r_c$ characterizes the deviation from the critical point. From the gap equation we can obtain the scaling of the mass and thus the exponent ν at the leading order. The leading m-dependent contribution for $m \to 0$ gives $m = 1/\xi \sim \tau$, which shows that the exponent $\nu = 1$ is no longer Gaussian.

V. THE 1/N CORRECTIONS

The large-N technique allows one to generate a systematic $1/N$ expansion. The evaluation of the Feynman rules shown in Fig. 3 is straightforward. Differentiating twice the action with respect to the shifted fields $\sigma_{1,2}$, defined as $\lambda_\alpha = im^2 + \sigma_\alpha$, $\alpha = 1, 2$, one obtains the σ_α-propagators, represented diagrammatically by dotted lines throughout the paper. At an intermediate step we find

$$S_2 = \frac{N}{2}\int_q \begin{pmatrix} \sigma_1(-q) & \sigma_2(-q) \end{pmatrix} \overleftrightarrow{\Delta}^{-1}(q) \begin{pmatrix} \sigma_1(q) \\ \sigma_2(q) \end{pmatrix}, \quad (20)$$

$$\overleftrightarrow{\Delta}^{-1}(q) = \begin{pmatrix} (\gamma^+ + \gamma^-)/2 + \frac{1}{2}\Pi(q) & (\gamma^+ - \gamma^-)/2 \\ (\gamma^+ - \gamma^-)/2 & (\gamma^+ + \gamma^-)/2 + \frac{1}{2}\Pi(q) \end{pmatrix}. \quad (21)$$

Taking the inverse of the 2×2 matrix we find the σ_i-propagators (i, $j = 1, 2$)

$$D_{ij}(q) = \frac{1}{N}\Delta_{ij}(q) = \frac{1}{2N}[\Delta_+(q,m) + (2\delta_{ij} - 1)\Delta_-(q,m)], \quad (22)$$

$$\Delta_\pm(q,m) = \frac{1}{\gamma_\pm + \frac{1}{2}\Pi(q)}, \quad (23)$$

$$\Pi(q) = \int_k \frac{1}{(k^2 + m^2)[(k+q)^2 + m^2]} = \frac{1}{4\pi q}\tan^{-1}(q/2m). \quad (24)$$

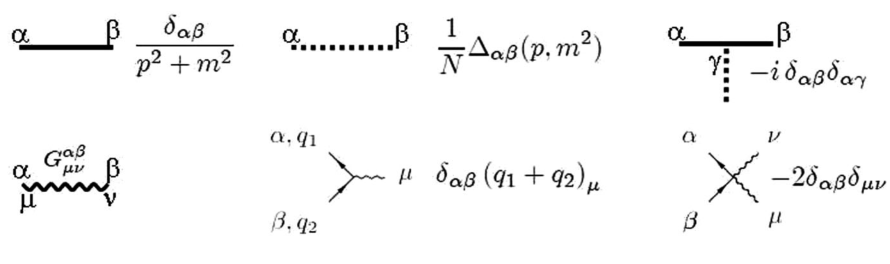

FIG. 3. Feynman rules for the $1/N$ expansion.

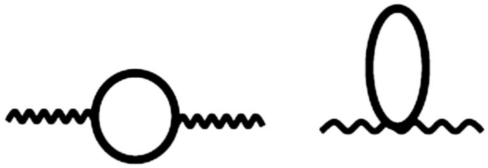

FIG. 4. One-loop diagrams that determine the effective action of the gauge fields at large N.

Similarly differentiating twice the large-N action with respect to the gauge fields and setting $\lambda_\alpha = im^2$, one obtains at an intermediate step

$$S_G^{(2)} = \frac{N}{4}\int_q a_\mu(-q)\left(\frac{q^2}{e_a^2} + \Gamma(q)\right)\delta^T_{\mu\nu}a_\nu(q) + b_\mu(-q)\left(\frac{q^2}{e_b^2} + \Gamma(q)\right)\delta^T_{\mu\nu}b_\nu(q) - 2\kappa b_\mu(-q)\epsilon_{\mu\lambda\nu}q_\lambda a_\nu(q). \tag{25}$$

Here, $\delta^T_{\mu\nu} = (\delta_{\mu\nu} - q_\mu q_\nu/q^2)$ and where the $\Gamma(q)$ term arises from the one-loop polarization diagrams shown in Fig. 4, which are expressed as

$$2\int_k \frac{\delta_{\mu\nu}}{k^2+m^2} - \int_k \frac{[2k_\mu + q_\mu][2k_\nu + q_\nu]}{(k^2+m^2)((k+q)^2+m^2)} = \Gamma(q)\delta^T_{\mu\nu}. \tag{26}$$

At zero temperature, a full analytic evaluation of the integrals is possible using the standard steps [13], and the result is

$$\Gamma(q) = \frac{q^2+4m^2}{8\pi q}\tan^{-1}\left(\frac{q}{2m}\right) - \frac{m}{4\pi}. \tag{27}$$

The resulting gauge propagators in Landau gauge are then $(\alpha, \beta = a, b)$

$$G^{\alpha\beta}_{\mu\nu}(q) = \frac{2}{N}[F_\alpha(q)\delta^T_{\mu\nu}\delta^{\alpha\beta} + G(q)\epsilon_{\mu\lambda\nu}q_\lambda(1-\delta^{\alpha\beta})], \tag{28}$$

$$F_a(q) = \frac{q^2/e_b^2 + \Gamma(q)}{(q^2/e_a^2 + \Gamma(q))(q^2/e_b^2 + \Gamma(q)) + q^2\kappa^2}, \tag{29}$$

$$G(q) = \frac{\kappa}{(q^2/e_a^2 + \Gamma(q))(q^2/e_b^2 + \Gamma(q)) + q^2\kappa^2}. \tag{30}$$

VI. CRITICAL EXPONENTS

Using the propagators derived in the previous section, we are now ready to compute two independent critical exponents associated with the singularity at the critical point (γ and η) including one-loop corrections about the $N = \infty$ saddle point. The critical exponent of interest ν is obtained from the scaling relation $\nu = \gamma/(2-\eta)$. We begin by calculating η, which is obtained from the two-point vertex function $\Gamma^{(2)}(p, m=0) = p^{2-\eta}$ by picking up the coefficient of the $p^2\ln p$. The self-energy diagrams that enter the two-point Ψ correlation function at order $1/N$ are diagrams (a) and (b) shown in Fig. 5. Their contribution gives

$$\Gamma^{(2)}(p, m=0) = p^2 + \frac{1}{N}\int_q \Delta_{11}(q)\left[\frac{1}{(q+p)^2} - \frac{1}{q^2}\right] - \frac{8}{N}\int_q \frac{p^2 - (p\cdot q)^2/q^2}{(q+p)^2}F_a(q). \tag{31}$$

In the critical region, $\Delta_{11}(q, m=0) \approx 16q$ and $F_a(q) \approx \Gamma(q)/[\Gamma^2(q) + q^2\kappa^2]$. Evaluating these diagrams asymptotically gives the divergent part

$$\Gamma^{(2)}(p, m=0) = p^2 + \frac{8}{3N\pi^2}p^2\ln(\Lambda/p) - \frac{128}{3N\pi^2}\frac{1}{1+c^2}\ln(\Lambda/p). \tag{32}$$

From this expression we read off the critical exponent η by re-exponentiating the p-terms

$$\eta = \frac{8}{3N\pi^2} - \frac{128}{3N\pi^2}\frac{1}{1+c^2} + o(1/N^2), \tag{33}$$

where $c = 16\kappa$. Consideration of two limiting cases of this result yields some expected results. First, it is consistent with the critical exponent η of the $O(N)$ symmetric scalar field model [6] when $c \to \infty$ corresponding to the decoupling of the gauge fields. Second, it is consistent with [14] when the Chern-Simons term is absent ($c = 0$).

The critical exponent γ determines how the mass of the scalar fields goes to zero at the critical point, i.e., $\Gamma^{(2)}(p=0, m) \sim m^\gamma$. The relevant self-energy diagrams that enter the two-point vertex function at order $1/N$ are all the diagrams shown in Fig. 5 [diagram (b) gives zero contribution when $p = 0$].

Evaluating these diagrams, we find

$$\Gamma^{(2)}(p=0,m) = m^2 + \frac{1}{N}\int_q \frac{\Delta_{11}(q)}{q^2+m^2} - \frac{\Delta_+(0,m)}{16\pi mN}\int_q \frac{\Delta_{11}(q)}{q^2+4m^2} + \frac{\Delta_+(0,m)}{2\pi N}\int_q F(q)\frac{\tan^{-1}(q/2m)}{q}. \tag{34}$$

Evaluating these integrals asymptotically gives the divergent part

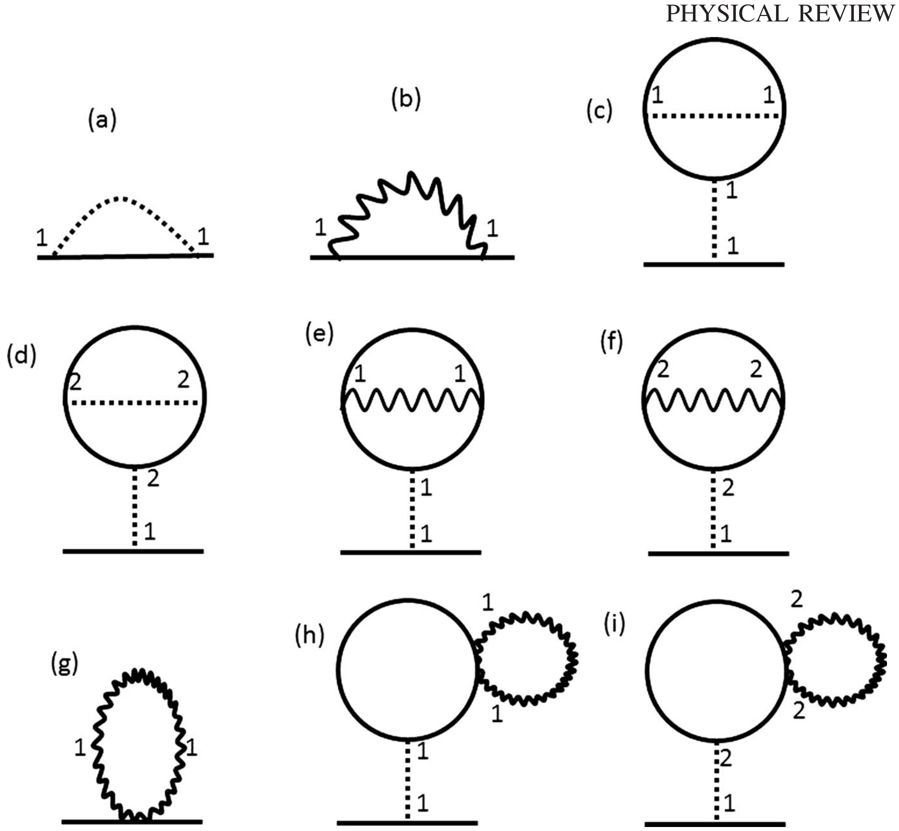

FIG. 5. Self-energy diagrams that enter the two-point scalar fields correlation function at order $1/N$.

$$\Gamma^{(2)}(p=0,m) = m^2 + \frac{24m^2}{N\pi^2}\ln\left(\frac{\Lambda}{m}\right) + \frac{128m^2(1-3c^2)}{N\pi^2(1+c^2)^2}\ln\left(\frac{\Lambda}{m}\right). \quad (35)$$

Re-exponentiating the logarithmic terms gives

$$\gamma = 2 - \frac{152}{N\pi^2} + \frac{128}{N\pi^2}\frac{c^2(c^2+5)}{(1+c^2)^2} + o(1/N^2). \quad (36)$$

We can now calculate the coefficient ν by using a scaling relation $\nu = \gamma/(2-\eta)$,

$$\nu = 1 - \frac{96}{N\pi^2} + \frac{256}{3N\pi^2}\frac{c^2(c^2+4)}{(1+c^2)^2} + o(1/N^2). \quad (37)$$

This result is consistent with the critical exponent ν of the $O(N)$ symmetric scalar field model [6] when one takes the limit $c \to \infty$ corresponding to the decoupling of the gauge fields. It is also consistent with the result of [14] when the Chern-Simons term is absent ($c = 0$).

VII. THE RENORMALIZED COUPLINGS

Using the propagators derived in the previous section, we now investigate the renormalized dimensionless zero-momentum four-point couplings $\hat{u}$ and $\hat{w}$ in the scaling region and obtain their fixed-point values for arbitrary N and at fixed dimension. We compute the relevant Feynman diagrams that contribute to the next-to-leading $1/N$ correction to the renormalized coupling as a function of the bare coupling and the renormalized mass. These are used to find the $1/N$ correction to the $\beta-$ functions $\beta(\hat{u}) = m_r d\hat{u}/dm_r$ and $\beta(\hat{w}) = m_r d\hat{w}/dm_r$ and the fixed-point values $\hat{u}^*$ and $\hat{w}^*$. Renormalization is performed according to the following prescription for the two- and four-point functions of the fields Ψ and Φ:

$$\Gamma^{(2)}_{11}(p) = \Gamma^{(2)}_{22}(p) = Z^{-1}[m_r^2 + p^2 + O(p^4)], \quad (38)$$

$$\Gamma^{(4)}_{1,1}(0,0,0,0) = Z^{-2}\frac{3\hat{u}}{N}m_r, \quad (39)$$

$$\Gamma^{(4)}_{1,2}(0,0,0,0) = Z^{-2}\frac{3\hat{w}}{N}m_r. \quad (40)$$

In terms of the self-energy $\Sigma(p,m)$ found from the diagrams in Fig. 5, the two-point function and the renormalized mass m_r are given by

$$\Gamma^{(2)}(p) = p^2 + m^2 - \Sigma(p,m), \quad (41)$$

$$m_r^2 = m^2 - \Sigma(0,m) + m^2\left[\frac{\partial\Sigma(p,m)}{\partial p^2}\right]_{p=0}. \quad (42)$$

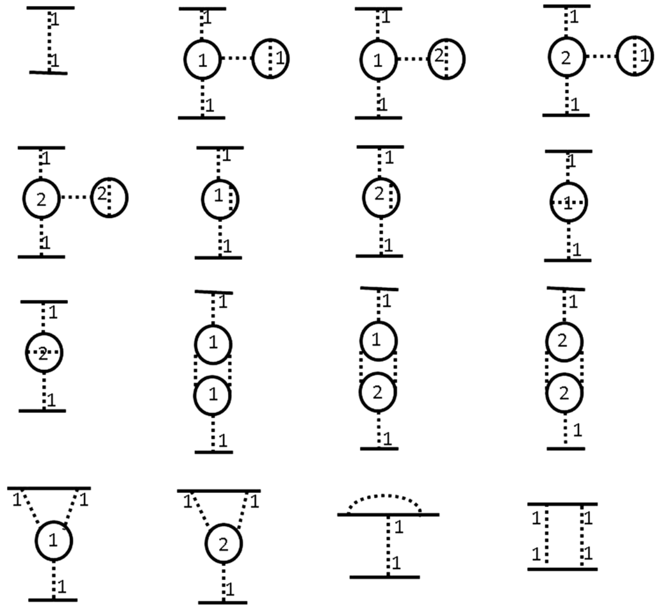

FIG. 6. Diagrammatic scalar field contributions to the four-point vertex function $\Gamma^{(4)}_{1,1}$.

The renormalized couplings $\hat{u}$ and $\hat{w}$ are given by

$$\hat{u} = \frac{N}{3m_r}\left[1 + 2\left[\frac{\partial\Sigma(p,m)}{\partial p^2}\right]_{p=0}\right]\Gamma^{(4)}_{1,1}(0,0,0,0), \quad (43)$$

$$\hat{w} = \frac{N}{3m_r}\left[1 + 2\left[\frac{\partial\Sigma(p,m)}{\partial p^2}\right]_{p=0}\right]\Gamma^{(4)}_{1,2}(0,0,0,0). \quad (44)$$

The relevant Feynman diagrams that contribute to the next-to-leading $1/N$ correction to $\Gamma^{(4)}_{1,1}$ and $\Gamma^{(4)}_{1,2}$ are, respectively, shown in Figs. 6–7 and Figs. 8–10.

In order to obtain finite results, $\hat{u}$ and $\hat{w}$ must be expressed in terms of the renormalized mass m_r. To achieve this, we express m in terms of m_r by inverting Eq. (42),

$$m^2 = m_r^2 + \Sigma(0,m_r) - m_r^2\left[\frac{\partial\Sigma(p,m_r)}{\partial p^2}\right]_{p=0} \quad (45)$$

and the scalar propagators at zero momentum are expressed as

$$D_{11}(0,m) = D_{11}(0,m_r) + \frac{D_{11}^2(0,m_r) + D_{12}^2(0,m_r)}{32\pi m_r^3} \times\left(\Sigma(0,m_r) - m_r^2\left[\frac{\partial\Sigma(p,m_r)}{\partial p^2}\right]_{p=0}\right), \quad (46)$$

$$D_{12}(0,m) = D_{12}(0,m_r) + \frac{D_{11}(0,m_r)D_{12}(0,m_r)}{16\pi m_r^3} \times\left(\Sigma(0,m_r) - m_r^2\left[\frac{\partial\Sigma(p,m_r)}{\partial p^2}\right]_{p=0}\right). \quad (47)$$

As a consequence, the divergences contained in the tadpole insertions (the first four tadpole diagrams in Fig. 6 and the first ten diagrams in Fig. 7) cancel out. In terms of the renormalized mass, we obtain the following representation of the renormalized couplings:

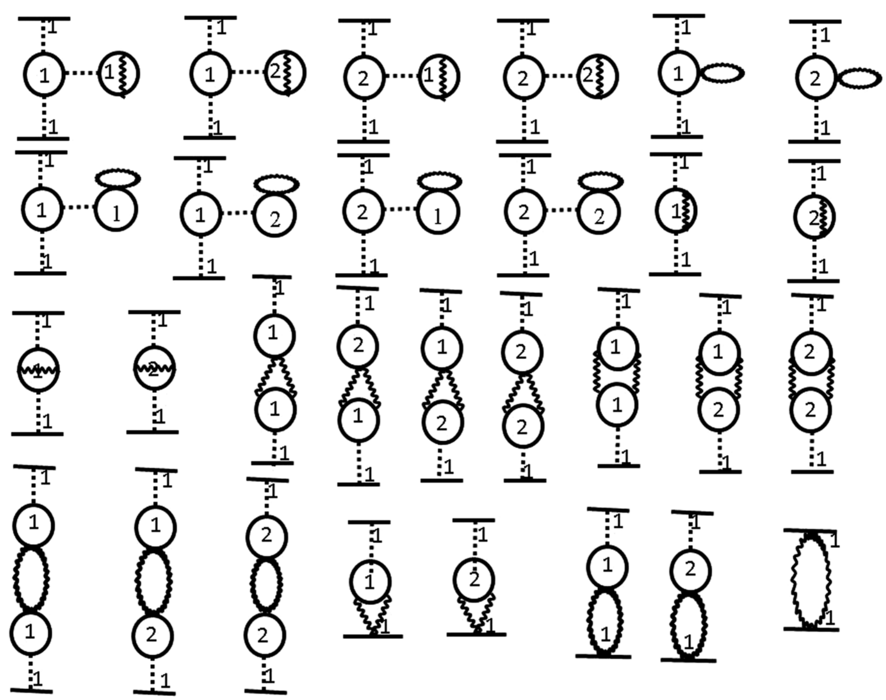

FIG. 7. Diagrammatic gauge field contributions to the four-point vertex function $\Gamma^{(4)}_{1,1}$.

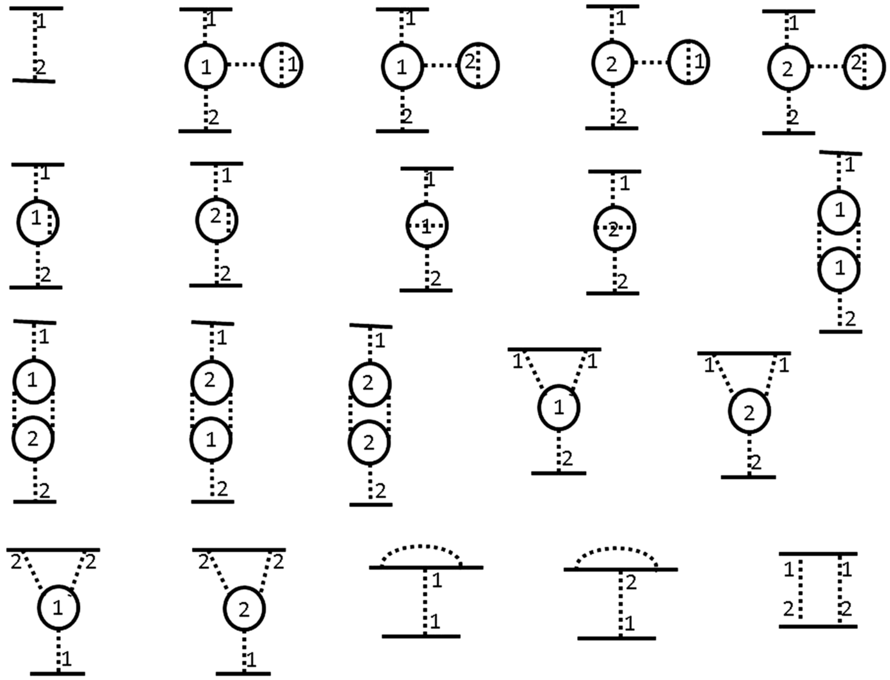

FIG. 8. Diagrammatic scalar field contributions to the four-point vertex function $\Gamma^{(4)}_{1,2}$.

$$
\begin{aligned}
m_r\hat{u} = {}& \Delta_{11}(0) - \frac{3}{4N}(2\Delta_{11}(0)-\delta_1)\int_q \frac{\Delta_{11}(q)}{(q^2+m_r^2)(q^2+4m_r^2)} - \frac{1}{2N}\left(5\Delta_{11}(0)+\frac{\delta_1}{6}\right)\int_q \frac{\Delta_{11}(q)}{(q^2+m_r^2)^2} + \frac{4}{N}\left(\Delta_{11}(0)-\frac{\delta_1}{2}\right) \\
&\times \int_q \frac{\Delta_{11}(q)}{(q^2+4m_r^2)^2} + \frac{2m_r^2}{N}\left(\Delta_{11}(0)+\frac{\delta_1}{6}\right)\int_q \frac{\Delta_{11}(q)}{(q^2+m_r^2)^3} - \frac{1}{2N}\int_q \frac{\Delta_+^2(q)+\Delta_-^2(q)}{(q^2+4m_r^2)^2}\left[\frac{3m_r^2}{q^2+m_r^2}+\gamma_+\Delta_+(0)\right]^2 \\
&- \frac{1}{N}\int_q \frac{\Delta_+(q)\Delta_-(q)}{(q^2+4m_r^2)^2}\left[\frac{3m_r^2}{q^2+m_r^2}+\gamma_-\Delta_-(0)\right]^2 + \frac{24m_r^2}{N}\left(\Delta_{11}(0)-\frac{\delta_1}{2}\right)\int_q \frac{F(q)}{(q^2+m_r^2)(q^2+4m_r^2)} + \frac{16\delta_1}{3N}\int_q \frac{F(q)}{q^2+m_r^2} \\
&- \frac{2\delta_1}{N\pi}\int_q F^2(q)\frac{\tan^{-1}(q/2m_r)}{q} + \frac{2\delta_2}{N\pi}\int_q qG^2(q)\tan^{-1}\left(\frac{q}{2m_r}\right) - \frac{8\delta_3}{N}\int_q F^2(q) + \frac{8\delta_4}{N}\int_q q^2G^2(q) \\
&- \frac{\Delta_{11}^2(0)+\Delta_{12}^2(0)}{4\pi^2N}\int_q F^2(q)\left[\frac{\tan^{-1}(q/2m_r)}{q}\right]^2 + \frac{\Delta_{11}(0)\Delta_{12}(0)}{2\pi^2N}\int_q G^2(q)\left[\tan^{-1}\left(\frac{q}{2m_r}\right)\right]^2 + O\left(\frac{1}{N^2}\right), \qquad (48)
\end{aligned}
$$

$$
\begin{aligned}
m_r\hat{w} = {}& \Delta_{12}(0) - \frac{3}{16\pi mN}\Delta_{11}(0)\Delta_{12}(0)\int_q \frac{\Delta_{11}(q)}{(q^2+m_r^2)(q^2+4m_r^2)} - \frac{\Delta_{12}(0)}{3N}\left(8-\frac{\Delta_{11}(0)}{16\pi m}\right)\int_q \frac{\Delta_{11}(q)}{(q^2+m_r^2)^2} \\
&+ \frac{1}{2\pi mN}\Delta_{11}(0)\Delta_{12}(0)\int_q \frac{\Delta_{11}(q)}{(q^2+4m_r^2)^2} + \frac{4m_r^2\Delta_{12}(0)}{3N}\left(2-\frac{\Delta_{11}(0)}{16\pi m}\right)\int_q \frac{\Delta_{11}(q)}{(q^2+m_r^2)^3} \\
&- \frac{1}{2N}\int_q \frac{\Delta_+^2(q)+\Delta_-^2(q)}{(q^2+4m_r^2)^2}\left[\frac{3m_r^2}{q^2+m_r^2}+\gamma_+\Delta_+(0)\right]^2 + \frac{1}{N}\int_q \frac{\Delta_+(q)\Delta_-(q)}{(q^2+4m_r^2)^2}\left[\frac{3m_r^2}{q^2+m_r^2}+\gamma_-\Delta_-(0)\right]^2 \\
&- \frac{\Delta_{11}(0)\Delta_{12}(0)}{\pi mN}\int_q \frac{F(q)}{(q^2+4m_r^2)} + \frac{16\Delta_{12}(0)}{3N}\left(2-\frac{\Delta_{11}(0)}{16\pi m}\right)\int_q \frac{F(q)}{q^2+m_r^2} - \frac{4\Delta_{12}(0)}{\pi N}\left(1-\frac{\Delta_{11}(0)}{8\pi m}\right) \\
&\times \int_q F^2(q)\frac{\tan^{-1}(q/2m_r)}{q} + \frac{4}{N\pi}\left(\Delta_{11}(0)-\frac{\Delta_{11}^2(0)+\Delta_{12}^2(0)}{16\pi m}\right)\int_q qG^2(q)\tan^{-1}\left(\frac{q}{2m_r}\right) + \frac{2\Delta_{12}(0)}{\pi mN}\left(1-\frac{\Delta_{11}(0)}{16\pi m}\right)\int_q F^2(q) \\
&+ \frac{16}{N}\left(1-\frac{\Delta_{11}(0)}{8\pi m}+\frac{\Delta_{11}^2(0)+\Delta_{12}^2(0)}{(16\pi m)^2}\right)\int_q q^2G^2(q) - \frac{\Delta_{11}(0)\Delta_{12}(0)}{4\pi^2N}\int_q F^2(q)\left[\frac{\tan^{-1}(q/2m_r)}{q}\right]^2 \\
&+ \frac{\Delta_{11}^2(0)+\Delta_{12}^2(0)}{4\pi^2}\int_q G^2(q)\left[\tan^{-1}\left(\frac{q}{2m_r}\right)\right]^2 + O\left(\frac{1}{N^2}\right), \qquad (49)
\end{aligned}
$$

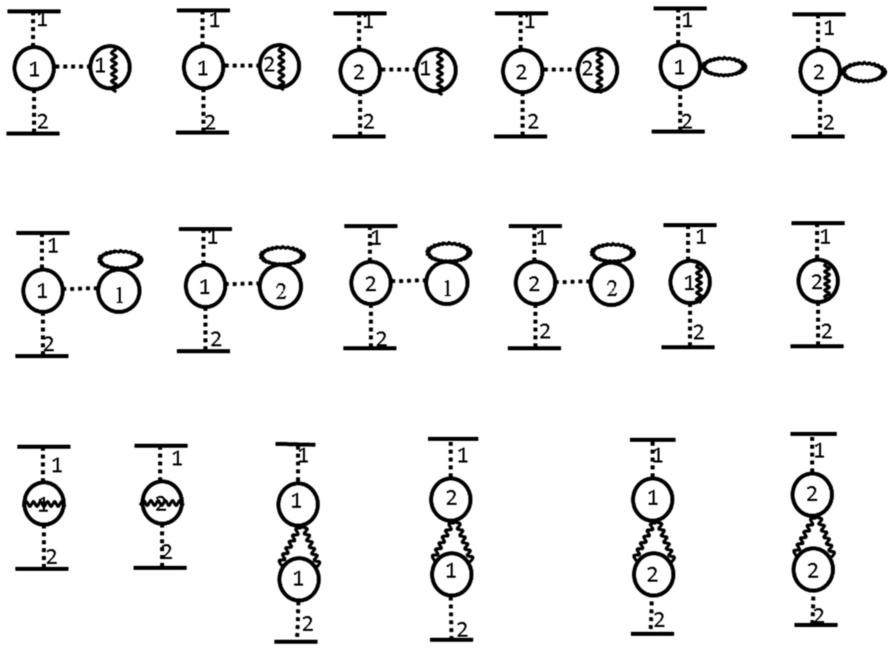

FIG. 9. Diagrammatic gauge field contributions to the four-point vertex function $\Gamma^{(4)}_{1,2}$.

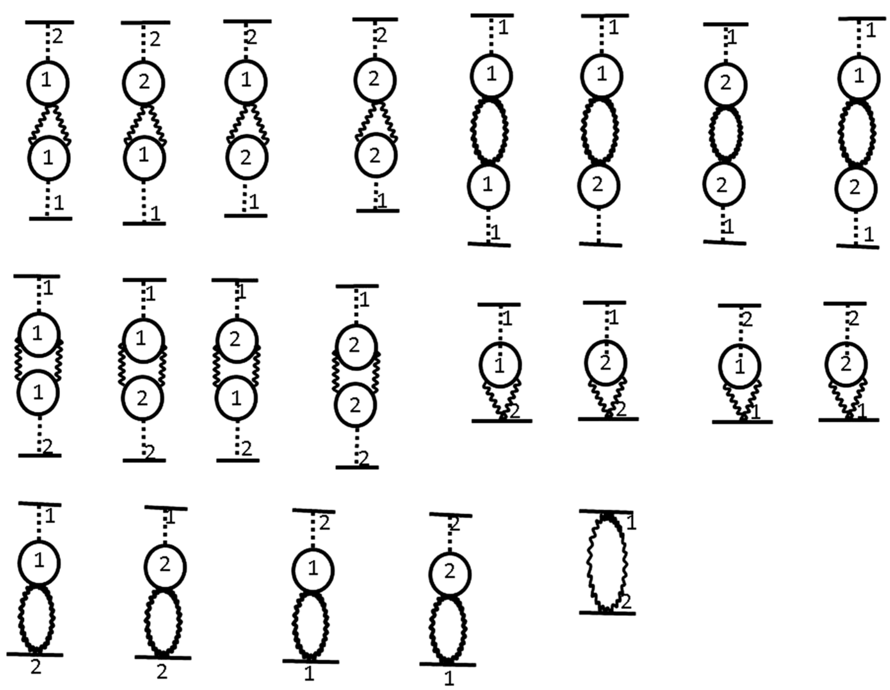

FIG. 10. Diagrammatic gauge field contributions to the four-point vertex function $\Gamma^{(4)}_{1,2}$.

where $\delta_1 = \gamma_+ \Delta_+^2(0) + \gamma_- \Delta_-^2(0)$; $\delta_2 = \gamma_+ \Delta_+^2(0) - \gamma_- \Delta_-^2(0)$; $\delta_3 = \gamma_+^2 \Delta_+^2(0) + \gamma_-^2 \Delta_-^2(0))$; $\delta_4 = \gamma_+^2 \Delta_+^2(0) - \gamma_-^2 \Delta_-^2(0)$.

We note that when $w = 0$ and in the absence of gauge fields Eq. (48) reduces to Eq. (24) of Ref [15] where an $O(N)$ invariant scalar field theory was considered. Of course the theory analyzed here is more complicated since it not only deals with two interacting multicomponent scalar fields, but it involves fluctuating gauge fields, too. By introducing a rescaled integration variable $x = q/m_r$, it becomes apparent that all the dependence on the renormalized mass and the bare couplings can only come through the dimensionless combinations $\hat{\gamma}_\pm = m_r \gamma_\pm$ and $\hat{e}^2 = e^2/m_r$. In the large-N limit, these equations reduce to

$$\hat{u} = 8\pi \left(\frac{1}{\hat{\gamma}_+ + 1} + \frac{1}{\hat{\gamma}_- + 1} \right), \tag{50}$$

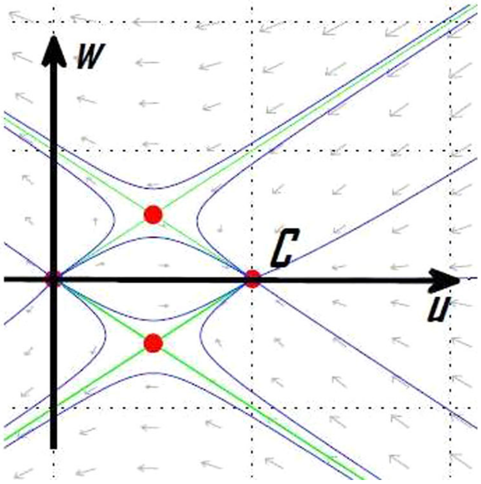

FIG. 11 (color online). The flow of the interaction coupling constants for $N = \infty$.

$$\hat{w} = 8\pi\left(\frac{1}{\hat{\gamma}_+ + 1} - \frac{1}{\hat{\gamma}_- + 1}\right) \tag{51}$$

and therefore the large-N limit of the β-functions reduce to

$$\beta_u^{(0)}(\hat{u},\hat{w}) = m_r\frac{d\hat{u}}{dm_r} = -\hat{u} + \frac{\hat{u}^2+\hat{w}^2}{16\pi}, \tag{52}$$

$$\beta_w^{(0)}(\hat{u},\hat{w}) = m_r\frac{d\hat{w}}{dm_r} = -\hat{w} + \frac{\hat{u}\,\hat{w}}{8\pi}. \tag{53}$$

These have four fixed points (see Fig. 11): $(\hat{u}_*,\hat{w}_*) = (0,0)$, the Gaussian fixed point, which is unstable in both directions in the $\hat{u}-\hat{w}$ plane; $(\hat{u}_*,\hat{w}_*) = (16\pi,0)$, the decoupled fixed point, which is stable; $(\hat{u}_*,\hat{w}_*) = (8\pi,8\pi)$, the enlarged $U(N)$ symmetric fixed point, which is unstable, and $(\hat{u}_*,\hat{w}_*) = (8\pi,-8\pi)$, which is also unstable.

The $1/N$ expanded β-functions of the model are constructed from Eqs. (48) and (49) by using the relations

$$\beta_u(\hat{u},\hat{w}) = m_r\frac{d\hat{u}}{dm_r} = \beta_u^{(0)}(\hat{u},\hat{w}) + \frac{1}{N}\beta_u^{(1)}(\hat{u},\hat{w}) + O\left(\frac{1}{N^2}\right), \tag{54}$$

$$\beta_w(\hat{u},\hat{w}) = m_r\frac{d\hat{w}}{dm_r} = \beta_w^{(0)}(\hat{u},\hat{w}) + \frac{1}{N}\beta_w^{(1)}(\hat{u},\hat{w}) + O\left(\frac{1}{N^2}\right). \tag{55}$$

To find expressions of the $O(1/N)$ contributions to the β-functions, it is convenient to work with the new coupling constants $\lambda_\pm = \hat{u} \pm \hat{w}$ that from Eqs. (48) and (49) can be expressed as

$$\lambda_\pm = \frac{16\pi}{\hat{\gamma}_\pm + 1} + \frac{1}{N}h_\pm(\hat{\gamma}_+,\hat{\gamma}_-,\hat{e}^2) + O\left(\frac{1}{N^2}\right) \tag{56}$$

and that lead to the following β-functions:

$$\beta_u(\hat{u},\hat{w}) = (\beta_{\lambda_+} + \beta_{\lambda_-})/2, \tag{57}$$

$$\beta_w(\hat{u},\hat{w}) = (\beta_{\lambda_+} - \beta_{\lambda_-})/2, \tag{58}$$

where

$$\beta_{\lambda_+} = m_r\frac{d\lambda_+}{dm_r} = \beta_{\lambda_+}^{(0)}(\lambda_+) + \frac{1}{N}[\beta_{\lambda_+}^{(0)}(\lambda_+)]^2\frac{\partial}{\partial\lambda_+}\left[\frac{h_+(\lambda_+,\lambda_-,\hat{e}^2)}{\beta_{\lambda_+}^{(0)}(\lambda_+)}\right] + \frac{1}{N}\beta_{\lambda_-}^{(0)}(\lambda_-)\frac{\partial h_+(\lambda_+,\lambda_-,\hat{e}^2)}{\partial\lambda_-} - \frac{\hat{e}^2}{N}\frac{\partial h_+(\lambda_+,\lambda_-,\hat{e}^2)}{\partial\hat{e}^2} + O\left(\frac{1}{N^2}\right), \tag{59}$$

$$\beta_{\lambda_-} = m_r\frac{d\lambda_-}{dm_r} = \beta_{\lambda_-}^{(0)}(\lambda_-) + \frac{1}{N}[\beta_{\lambda_-}^{(0)}(\lambda_-)]^2\frac{\partial}{\partial\lambda_-}\left[\frac{h_-(\lambda_+,\lambda_-,\hat{e}^2)}{\beta_{\lambda_-}^{(0)}(\lambda_-)}\right] + \frac{1}{N}\beta_{\lambda_+}^{(0)}(\lambda_+)\frac{\partial h_-(\lambda_+,\lambda_-,\hat{e}^2)}{\partial\lambda_+} - \frac{\hat{e}^2}{N}\frac{\partial h_-(\lambda_+,\lambda_-,\hat{e}^2)}{\partial\hat{e}^2} + O\left(\frac{1}{N^2}\right), \tag{60}$$

$$\beta_{\lambda\pm}^{(0)}(\lambda_\pm) = -\lambda_\pm\left(1 - \frac{\lambda_\pm}{16\pi}\right). \tag{61}$$

Regarding the fixed-point values of $\hat{u}$ and $\hat{w}$, these can be easily obtained directly from Eqs. (48)–(49) by taking the limit $\hat{\gamma}_\pm \to 0$ and $\hat{e}^2 \to \infty$ and evaluating the remaining integrals. The result in integral form is

$$\frac{\hat{u}^*}{16\pi} = 1 - \frac{4\pi}{N}\int\frac{d^3x}{(2\pi)^3}\frac{x}{\arctan(x/2)(x^2+1)^2}\left(\frac{8}{x^2+1} + \frac{9}{x^2+4}\right) + \frac{24}{N}\int\frac{d^3x}{(2\pi)^3}\frac{\Omega(x)}{(\Omega^2(x)+x^2\kappa^2)(x^2+1)(x^2+4)} - \frac{4}{N\pi}\int\frac{d^3x}{(2\pi)^3}\left[\frac{\Omega(x)\arctan(x/2)}{x(\Omega^2(x)+x^2\kappa^2)}\right]^2, \tag{62}$$

$$\hat{w}^* = \frac{64\kappa^2}{N}\int\frac{d^3x}{(2\pi)^3}\left[\frac{\arctan(x/2)}{\Omega^2(x)+x^2\kappa^2}\right]^2, \tag{63}$$

where $\Omega(x) = (x^2+4)\tan^{-1}(x/2)/(8\pi x) - 1/4\pi$. Numerical evaluation of these integrals for the relevant value $\kappa = 1/\pi$ gives $\hat{u}^* = 16\pi(1 - 3.545/N)$ and $\hat{w}^* = 34/N$.

VIII. CONDUCTIVITY NEAR THE CRITICAL POINT

It is interesting to examine the conductivity near the quantum critical point. This may be computed as the response of the system to a weak external electromagnetic field A_μ. Since the charged bosons in the system are Cooper pairs whose current is $p_\mu = (1/\pi)\epsilon^{\mu\nu\lambda}\partial_\nu b_\lambda$, the probing electromagnetic field A_μ will enter the partition function through the term $2eA_\mu J_\mu = \frac{2e}{\pi} A_\mu \epsilon^{\mu\nu\lambda}\partial_\nu b_\lambda$ in Eq. (3). The effective action of the external electromagnetic gauge fields A_μ is obtained after integrating out the fluctuations in b_μ, a_μ, resulting in $S_{\rm eff}[A_\mu] = 1/2 \int A_\mu(-q)K_{\mu\nu}(q)A_\nu(q)$ where $K_{\mu\nu}(q) = (2e/\pi)^2 \epsilon^{\mu\tau\beta}\epsilon^{\nu\rho\alpha} q_\alpha q_\beta \langle b_\tau(-q)b_\rho(q)\rangle$. The resulting conductivity (per flavor) is $\sigma_{ij}(\omega) = K_{ij}(\mathbf{q} = 0, \omega)/\omega = \sigma(\omega)\delta_{ij}$ with

$$\sigma(\omega) = \frac{2\omega}{\pi R_q} \frac{\omega^2/e_a^2 + \Gamma(\omega)}{(\omega^2/e_a^2 + \Gamma(\omega))(\omega^2/e_b^2 + \Gamma(\omega)) + \omega^2\kappa^2}; \tag{64}$$

here, $R_q = 2\pi\hbar/4e^2$ is the quantum resistance for Cooper pairs. Near the critical region, this reduces to

$$\sigma(\omega) = \frac{1}{R_q} f\left(\frac{\omega}{m}\right), \tag{65}$$

$$f(x) = \frac{2}{\pi} \frac{x\Omega(x)}{\Omega^2(x) + x^2\kappa^2}. \tag{66}$$

At the critical point $m = 0$, the conductivity is a universal number

$$\sigma^* = \frac{\pi}{8R_q} \frac{1}{1 + \pi^2/16^2}. \tag{67}$$

This is the leading (zeroth) order in $1/N$ expansion. To obtain the first order correction to the universal conductivity in the $1/N$ expansion, we need the corrections to the propagators of the gauge fields a_μ and b_μ, Eq. (28), by adding new diagrams constructed by substituting complex scalar loops to each vertex in diagrams of Fig. 4 and attaching to it the propagators in all possible ways. The needed diagrams are shown in Figs. 12–13.

The tadpole insertion diagrams in Fig. 12 cancel out once we express the leading order polarization tensor in Eq. (26) in terms of the renormalized mass in Eq. (42):

$$\Gamma(q, m) = \Gamma(q, m_r) + \frac{1}{2\pi}\left[\Sigma(0, m_r) - m_r^2 \left[\frac{\partial\Sigma(p, m_r)}{\partial p^2}\right]_{p=0}\right] \times \left[\frac{2m_r}{q}\arctan\left(\frac{q}{2m_r}\right) - 1\right]. \tag{68}$$

The other graphs in Fig. 13 contribute to the $1/N$ correction to the polarization tensor. Gauge invariance is preserved since each internal gauge field propagator is combined with its corresponding seagull diagram. As we show in Appendix A, diagrams (1) and (2) combine to give a finite and transverse contribution to the polarization tensor. Similarly, the combination of diagrams (3), (4), (5), and (6) is finite and transverse. Finally, diagrams (7), (8), and (9) combine to give also a finite and a transverse contribution. The result is a transverse polarization tensor $\Pi_{\mu\nu}(q) = \Pi(q)\delta^T_{\mu\nu}$. The resulting momentum integrals at the critical point ($m_r = 0$) are presented in Appendix A. It is important to note that at the critical point the contribution to the mixed Chern-Simons term at the $1/N$ order is zero. This is because such a contribution could only result from diagrams with two loops like diagram (8) involving an internal scalar field propagator $D_{12}(q)$. However, such a propagator is proportional to $\hat\gamma_+ - \hat\gamma_-$ and hence gives zero contribution at the critical point. This is consistent with a known fact that in a topological field theory the Chern-Simons term does not renormalize [13]. The b_μ-gauge propagator at the critical point ($m_r = 0$) including corrections to the leading order in $1/N$ is then

$$\langle b_\mu(-q)b_\nu(q)\rangle = \frac{\Gamma(q) - \Pi(q)/N}{(\Gamma(q) - \Pi(q)/N)^2 + q^2\kappa^2}\delta^T_{\mu\nu}, \tag{69}$$

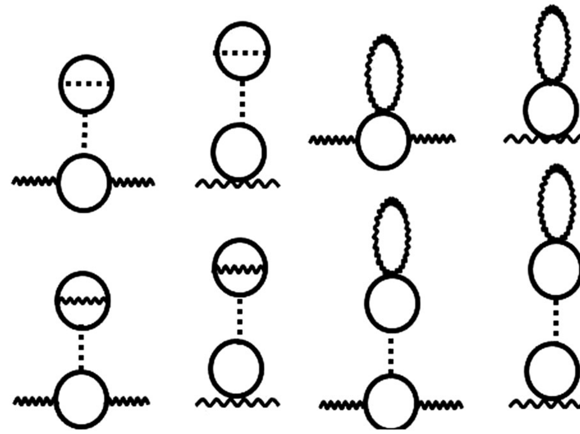

FIG. 12. Contributions with tadpole insertion to the vacuum polarization tensor to order $1/N$.

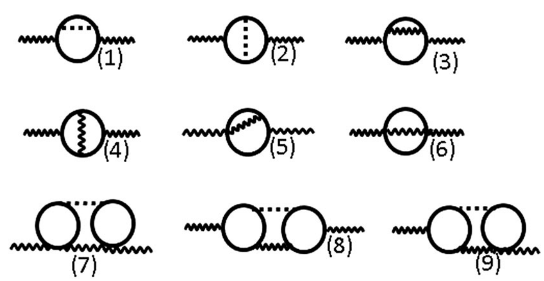

FIG. 13. Contributions to the vacuum polarization tensor to order $1/N$.

where $\Pi(q) = 4q/(9\pi^2) - 2q(7/3\pi^2 + 0.11)/(1 + c^2)$. The resulting universal dc conductivity to $O(1/N)$ is

$$\sigma = \sigma^*\left(1 + \frac{1}{N}\frac{c^2-1}{c^2+1}\left[-\frac{64}{9\pi^2} + \frac{32}{c^2+1}\left(\frac{7}{3\pi^2} + 0.11\right)\right]\right). \tag{70}$$

For Josephson junction array systems $N = 2$, this yields $\sigma = 0.21(2e)^2/h$. Thus, the next-to-leading order correction to the universal conductivity in the $1/N$ expansion reduces the value by about 14%.

IX. CONCLUSION

In summary, the critical behavior of a $U(N/2) \times U(N/2)$ Ginzburg-Landau theory containing two multicomponent complex fields coupled to gauge fields described by Maxwell terms and a Mixed-Chern-Simons term was investigated in the framework of the $1/N$ expansion at fixed dimension $d = 3$. The critical exponents ν, η, and γ are calculated to the $O(1/N)$. We computed the dependence of the renormalized zero-momentum four-point quartic couplings $\hat{u}$ and $\hat{w}$ from the renormalized mass m_r and the bare couplings to order $O(1/N)$. The resulting beta functions and the fixed-point values of the couplings were also obtained within the same approximation. In the limit of an $O(N)$ invariant scalar field theory ($w = 0$ and no fluctuating gauge fields) our result for the fixed-point value of the coupling u agrees with that of [15]. For nonzero four-point quartic couplings $\hat{u}$ and $\hat{w}$, it is found that the decoupled fixed point that was stable within the approximate one-loop renormalization group for $N > 4$ is destabilized in the framework of the $1/N$ expansion since $\hat{w}^* \neq 0$. This is attributed to the interaction mediated by the mixed Chern-Simons term. The dc conductivity that includes corrections to the leading order in $1/N$ is found to be universal. It is important to note here that the universal conductivity is obtained when both chargelike and magneticlike modes are simultaneously excited and when both fluctuating gauge fields are taken into account. In this regard our result is more general than that of [16], which considered the dynamics of a single complex field (representing chargelike modes only) and in the absence of fluctuating gauge fields. Furthermore, here we recover the result of [16] in the limit of extremely massive magnetic modes. In fact in this case the Φ field decouples form the theory and the gauge field b_μ now essentially plays the role of a Lagrange multiplier that imposes the constraint $a_\mu = -2eA_\mu$ where the probing electromagnetic field A_μ enters the Lagrangian in Eq. (3) through the term $2eA_\mu J_\mu = \frac{2e}{\pi}A_\mu\epsilon^{\mu\nu\lambda}\partial_\nu b_\lambda$. The resulting effective action reduces then to the standard Landau–Ginzburg theory considered in [16] with only chargelike modes Ψ coupled to A_μ. In this case the next-to-leading order correction to the conductivity involves only diagrams (1) and (2) in Fig. 13 and the result is

$$\sigma = \frac{\pi}{8R_q}\left(1 - \frac{64}{9\pi^2 N}\right), \tag{71}$$

which reproduces Eq. (5.25) of [16] (note that here $N/2 = M$).

It would be interesting to investigate higher corrections to the conductivity at finite temperature when chargelike and magneticlike modes are simultaneously excited. This effect is known to involve crossover phenomena between different dimensions when the temperature varies from zero to infinity. Large-N technique is particularly well suited to study such a crossover situation. We hope to tackle these points in future works.

ACKNOWLEDGMENTS

The author thanks Gordon Semenoff and Igor F. Herbut for valuable discussions. I acknowledge the hospitality of the physics department at UBC and at SFU where part of this research was carried out. This work was supported by AUS Grant No. FRG3.

APPENDIX A: EVALUATION OF THE POLARIZATION TENSOR TO ORDER 1/N

In this appendix, we provide more details on how we evaluate the momentum integrals appearing in the two- and three-loop diagrams for the gauge propagator to order $1/N$ at the critical point. We show that all momentum-dependent singularities from different diagrams mutually cancel to $1/N$ and that the polarization tensor is transverse. Most calculations at order $1/N$ rely on the evaluation of the generic d-dimensional integrals

$$\int_k \frac{1}{(k+p)^{2\alpha}k^{2\beta}} = p^{d-2\alpha-2\beta}\frac{\Gamma(\alpha+\beta-d/2)\Gamma(d/2-\alpha)\Gamma(d/2-\beta)}{(4\pi)^{d/2}\Gamma(\alpha)\Gamma(\beta)\Gamma(d-\alpha-\beta)}, \tag{A1}$$

$$\int_k \frac{k_\mu}{(k+p)^{2\alpha}k^{2\beta}} = -p_\mu p^{d-2\alpha-2\beta}\frac{\Gamma(\alpha+\beta-d/2)\Gamma(d/2-\alpha)\Gamma(d/2-\beta+1)}{(4\pi)^{d/2}\Gamma(\alpha)\Gamma(\beta)\Gamma(d-\alpha-\beta+1)}, \tag{A2}$$

$$\int_k \frac{k_\mu k_\nu}{(k+p)^{2\alpha}k^{2\beta}} = \frac{p^{d+2-2\alpha-2\beta}}{(4\pi)^{d/2}\Gamma(\alpha)\Gamma(\beta)\Gamma(d-\alpha-\beta+2)}\left\{\frac{1}{2}\delta_{\mu\nu}\Gamma(\alpha+\beta-d/2-1)\Gamma(d/2-\alpha+1)\Gamma(d/2-\beta+1) + \frac{p_\mu p_\nu}{p^2}\Gamma(\alpha+\beta-d/2)\Gamma(d/2-\alpha)\Gamma(d/2-\beta+2)\right\}. \tag{A3}$$

In what follows $d = 3 - \epsilon$, and the singularities appear as poles in $1/\epsilon$. If one chooses a hard cutoff and restricts the integration to values $k \leq \Lambda$, the residue of the pole yields the coefficient of $p \ln(\Lambda/p)$. The expression of the first diagram with a scalar self-energy correction is

$$\Pi^{(1)}_{\mu\nu}(p) = -8 \int_{k,q} \frac{[2k_\mu + p_\mu][2k_\nu + p_\nu]q}{k^4(k+p)^2} \left[\frac{1}{(k+q)^2} - \frac{1}{q^2}\right]. \tag{A4}$$

The integration over q is done first with the intermediate result

$$\Pi^{(1)}_{\mu\nu} = -\frac{4}{3\pi^2}\left(\frac{1}{\epsilon} - \frac{\gamma}{2} - \ln(2) + \frac{8}{3}\right) \int_k \frac{[2k_\mu + p_\mu][2k_\nu + p_\nu]}{k^{2+\epsilon}(k+p)^2}. \tag{A5}$$

Next, the integration over k is done with the result

$$\Pi^{(1)}_{\mu\nu}(p) = \frac{p}{12\pi^2}\left[\left(\frac{1}{\epsilon} + \frac{47}{12} - \gamma\right)\delta^T_{\mu\nu}(p) + \frac{1}{2}\frac{p_\mu p_\nu}{p^2}\right]. \tag{A6}$$

The expression of the second diagram with a scalar vertex correction is

$$\Pi^{(2)}_{\mu\nu}(p) = -8 \int_{k,q} \frac{q[2k_\mu + p_\mu][2k_\nu + 2q_\nu + p_\nu]}{k^2(k+p)^2(k+q)^2(k+p+q)^2}. \tag{A7}$$

We find it useful to decompose this polarization tensor in terms of its transverse part and its longitudinal part

$$\Pi^{(2)}_{\mu\nu}(p) = \Pi_t(p)\delta^T_{\mu\nu}(p) + \Pi_L(p)\frac{p_\mu p_\nu}{p^2}. \tag{A8}$$

The integral giving the longitudinal part can be reduced by means of the formula

$$2k \cdot p = (k+p)^2 - p^2 - k^2 \tag{A9}$$

and, after performing the q integration, the intermediate integral is

$$\Pi^{(2)}_L(p) = -\frac{8}{3\pi^2 p^2}\left(\frac{1}{\epsilon} - \frac{\gamma}{2} - \ln(2) + \frac{8}{3} + O(\epsilon)\right) \times \int_k \frac{p^2 + 2k\cdot p}{k^\epsilon (k+p)^2}. \tag{A10}$$

Next, the integration over k is done with the result

$$\Pi^{(2)}_L(p) = -\frac{p}{12\pi^2}. \tag{A11}$$

To get the transverse part of $\Pi^{(2)}_{\mu\nu}(p)$, we first find the trace $\Pi^{(2)\mu}_\mu(p)$ and use the relation $\Pi^{(2)\mu}_\mu(p) = (d-1)\Pi_t(p) + \Pi_L(p)$. Repeated use of formula (A9) gives

$$\Pi^{(2)\mu}_\mu(p) = -8 \int_{k,q} \frac{4q}{k^2(k+p)^2(k+q)^2} - \frac{q(2q^2+p^2)}{k^2(k+p)^2(k+q)^2(k+p+q)^2}. \tag{A12}$$

The first part in (A12) is easily done by integrating first over q using the generic formula (A1) followed by another generic k-integration. The second part in (A12) requires more work and is of the generic form

$$\int_{k_1,k_2} \frac{1}{k_1^{2n_1} k_2^{2n_2} (k_1+p)^{2n_3}(k_2+p)^{2n_4}(k_1-k_2)^{2n_5}} = p^{2d-\Sigma n_i} G(n_1, n_2, n_3, n_4, n_5). \tag{A13}$$

These types of integrals are handled by finding recurrence relations (known as triangle relations) for $G(n_1, n_2, n_3, n_4, n_5)$, which are obtained by applying the operators $\partial_1 \cdot (k_1 - k_2)$ and $\partial_1 \cdot k_1$ to the integrand of (A13). Relevant to the integrals needed in (A12), these relations are

$$(d-3)G(1,1,1,1,1/2) + (2d-5)G(1,1,1,1,-1/2) = f(-1/2), \tag{A14}$$

$$(d-1)G(1,1,1,1,-1/2) + (2d-3)G(1,1,1,1,-3/2) = f(-3/2), \tag{A15}$$

where

$$f(n_5) = 2(G(2,n_5)G(1, 3+n_5-d/2) - G(1,n_5+1)G(2,n_5+3-d/2), \tag{A16}$$

$$G(n,m) = \frac{\Gamma(n+m-d/2)\Gamma(d/2-n)\Gamma(d/2-m)}{(4\pi)^d\Gamma(n)\Gamma(m)\Gamma(d-n-m)}. \tag{A17}$$

The resulting transverse part is

$$\Pi^{(2)}_t(p) = -\frac{p}{6\pi^2\epsilon} - \frac{31}{72\pi^2} + \frac{\gamma p}{6\pi^2}. \tag{A18}$$

Adding the two polarization tensors with corrections from the scalar field self-energy and vertex contributions, taking into account a combinatorial factor 2 for the self-energy diagram, gives

$$2\Pi^{(1)}_{\mu\nu}(p) + \Pi^{(2)}_{\mu\nu}(p) = \frac{2p}{9\pi^2}\delta^T_{\mu\nu}(p). \tag{A19}$$

We verify that the two longitudinal components and the $1/\epsilon$ singularities in the transverse parts both sum to 0 as they should.

Next, we proceed to evaluate the diagrams with gauge field propagators. We find it convenient to combine directly diagrams (3) and (5) as the logarithmic singularities in each diagram cancel out and their combination gives a finite contribution to the polarization tensor. We verified that both calculations using a hard cutoff and dimensional regularization give the same answer,

$$\text{diagram}(3)+(5) = 2\int_{k,q}\frac{[2k_\mu+p_\mu][2k_\nu+p_\nu]}{k^4(k+p)^2}\frac{[2k_\lambda+q_\lambda]G_{\lambda\tau}(q)[2k_\tau+q_\tau]}{(k+q)^2} - 4\int_{k,q}\frac{[2k_\nu+p_\nu][2k_\tau+q_\tau]}{k^2(k+p)^2}\frac{G_{\mu\tau}(q)}{(k+q)^2}+(\mu\leftrightarrow\nu). \tag{A20}$$

Note the factors 2 and 4 in front of each integral, which account for the fact that there are two self-energy insertions for the diagram of type (3) and the two diagrams of type (5), each has a factor -2 at the vertex where two gauge field lines meet. We first perform a generic integration over q, and, simplifying the combined integrands, we get at an intermediate step

$$\text{diagram}(3)+(5) = -\frac{128}{3\pi^2(1+c^2)}\int_k \ln(k)\frac{k_\mu p_\nu+p_\mu k_\nu+p_\mu p_\nu}{k^2(k+p)^2}. \tag{A21}$$

It is easy to check that the trace $\Pi_\mu^{(3+5)\mu}(p)$ and the longitudinal part are given by the same integral. As a result, the transverse part is zero.

The remaining k-integration can be done easily, resulting in

$$\Pi_{\mu\nu}^{(3+5)}(p) = \frac{8p}{3\pi^2(1+c^2)}\frac{p_\mu p_\nu}{p^2}. \tag{A22}$$

The diagram (4) with a gauge field vertex correction is expressed by the following integral:

$$\Pi_{\mu\nu}^{(4)}(p) = \int_{k,q}\frac{[2k_\mu+p_\mu][2k_\nu+2q_\nu+p_\nu][2k_\lambda+q_\lambda]G_{\lambda\tau}(q)[2k_\tau+2p_\tau+q_\tau].}{k^2(k+p)^2(k+q)^2(k+p+q)^2} \tag{A23}$$

It is finite. Its longitudinal part $\Pi_L^{(4)}(p) = p_\mu\Pi_{\mu\nu}^{(4)}(p)p_\nu/p^2$ can be easily obtained by using formula (A9) and then performing the q-integration using (A1–A3),

$$\Pi_L^{(4)}(p) = -\frac{2p}{3\pi^2(1+c^2)}. \tag{A24}$$

Its transverse part is finite, but it requires more work. We first find its trace $\Pi_\mu^{(4)\mu}(p)$ and make use repeatedly of formula (A9). This generates several terms in the integrand that can be computed easily with the help of (A1) and one term that is of the type (A13). At an intermediate step, we get

$$\Pi_\mu^{(4)\mu}(p) = \frac{1}{1+c^2}\left(-\frac{70p}{9\pi^2}+32p^4G(1,1,1,1,1/2)\right) = -\frac{1}{1+c^2}\left(\frac{70p}{9\pi^2}+\frac{4p}{\pi^2}\left(\frac{\pi^2}{12}+\frac{1}{2}\ln(1+\sqrt{2})\times\ln(2+2\sqrt{2})+di\log(1+\sqrt{2})+di\log(2+\sqrt{2})\right)\right). \tag{A25}$$

$G(1,1,1,1,1/2)$ is the integral defined in (A13) (see Appendix C for its computation). The resulting transverse part is

$$\Pi_T^{(4)}(p) = -\frac{1}{1+c^2}\left(\frac{32p}{9\pi^2}+\frac{p}{6}+\frac{2p}{\pi^2}\times\left(\frac{1}{2}\ln(1+\sqrt{2})\ln(2+2\sqrt{2})+di\log(1+\sqrt{2})+di\log(2+\sqrt{2})\right)\right). \tag{A26}$$

Diagram (6) is expressed by the following integral:

$$\Pi_{\mu\nu}^{(6)}(p) = 4\int_{k,q}\frac{G_{\mu\nu}(q)}{(k+p)^2(k+q)^2}. \tag{A27}$$

This is easily computed with the use of (A1)–(A3) and the result is

$$\Pi_{\mu\nu}^{(6)}(p) = -\frac{p}{\pi^2(1+c^2)}\left(\delta_{\mu\nu}+\frac{p_\mu p_\nu}{p^2}\right). \tag{A28}$$

Note that when diagrams (3), (4), (5), and (6) are added the result is transverse. This is the same as in the two-loop diagrams of scalar QED_3; the only difference is the form of the internal gauge propagator.

$$\Pi^{(3)}_{\mu\nu}(p)+\Pi^{(4)}_{\mu\nu}(p)+\Pi^{(5)}_{\mu\nu}(p)+\Pi^{(6)}_{\mu\nu}(p) = -\frac{p}{\pi^2(1+c^2)}\left(\delta_{\mu\nu}-\frac{p_\mu p_\nu}{p^2}\right)\left(\frac{41}{9}+\frac{\pi^2}{6}+\ln(1+\sqrt{2})\ln(2+2\sqrt{2}) + 2di\log(1+\sqrt{2})+2di\log(2+\sqrt{2})\right)$$
$$= -\frac{p}{(1+c^2)}\left(\delta_{\mu\nu}-\frac{p_\mu p_\nu}{p^2}\right)\left(\frac{1}{\pi^2}+0.1102531\right). \quad (A29)$$

Diagram (7) is expressed by the following integral:

$$\Pi^{(7)}_{\mu\nu}(p) = -4\int_{k,q,l}\frac{G_{\mu\nu}(q)D(p+q)}{k^2(k+p+q)^2 l^2(l+p+q)^2}. \quad (A30)$$

With the help of (A1) we first perform the two separate integrations over k and over l; then with the help of (A3) we compute the resulting integration over q. The result is

$$\Pi^{(7)}_{\mu\nu}(p) = \frac{p}{\pi^2(1+c^2)}\left[\delta_{\mu\nu}+\frac{p_\mu p_\nu}{p^2}\right]. \quad (A31)$$

It is important to notice that when diagrams (7), (8), and (9) are combined, the resulting tensor is transverse and its expression is convergent. Gauge invariance is preserved since each gauge propagator is combined with its seagull diagram. Diagram (8) is expressed by the following integral:

$$\Pi^{(8)}_{\mu\nu}(p) = -4\int_{k,q,l}\frac{[2k_\mu+p_\mu][2l_\nu+p_\nu][2k_\lambda+q_\lambda][2l_\tau+q_\tau]G_{\lambda\tau}(q)D(p-q)}{k^2(k+p)^2(k+q)^2 l^2(l+p)^2(l+q)^2}. \quad (A32)$$

Diagram (9) is given by

$$\Pi^{(9)}_{\mu\nu}(p) = 4\int_{k,q,l}\frac{[2l_\nu+p_\nu]}{k^2(k+p+q)^2}\left[\frac{[2l_\tau-q_\tau]}{l^2(l+p)^2(l-q)^2}+\frac{[2l_\tau+2p_\tau+q_\tau]}{l^2(l+p)^2(l+p+q)^2}\right] \times G_{\mu\tau}(q)D(p+q). \quad (A33)$$

With the help of the following formulas (see Appendix B for their derivation),

$$\int_k \frac{k_\mu}{k^2(k+p)^2(k+q)^2} = -\frac{1}{8|\mathbf{p}-\mathbf{q}|(p+q+|\mathbf{p}-\mathbf{q}|)}\left(\frac{p_\mu}{p}+\frac{q_\mu}{q}\right), \quad (A34)$$

$$\int_k \frac{k_\mu k_\nu}{k^2(k+p)^2(k+q)^2} = A\delta_{\mu\nu}+Bp_\mu p_\nu + C(p_\mu q_\nu+q_\mu p_\nu)+Dq_\mu q_\nu, \quad (A35)$$

$$A=\frac{1}{16(p+q+|\mathbf{p}-\mathbf{q}|)},\qquad B=\frac{p+2q+|\mathbf{p}-\mathbf{q}|}{16p|\mathbf{p}-\mathbf{q}|(p+q+|\mathbf{p}-\mathbf{q}|)^2}, \quad (A36)$$

$$C=\frac{1}{16|\mathbf{p}-\mathbf{q}|(p+q+|\mathbf{p}-\mathbf{q}|)^2},\qquad D=\frac{2p+q+|\mathbf{p}-\mathbf{q}|}{16q|\mathbf{p}-\mathbf{q}|(p+q+|\mathbf{p}-\mathbf{q}|)^2}. \quad (A37)$$

The two separate integrations over k and over l in $\Pi^{(8)}_{\mu\nu}(p)$ yield

$$\Pi^{(8)}_{\mu\nu}(p) = -\frac{32}{(1+c^2)}\int_q \frac{q}{|\mathbf{p}-\mathbf{q}|(p+q+|\mathbf{p}-\mathbf{q}|)^4}\left(|\mathbf{p}-\mathbf{q}|(p+q+|\mathbf{p}-\mathbf{q}|)\frac{\delta_{\mu\lambda}}{q}+\frac{p_\mu p_\lambda}{p}+\frac{q_\mu p_\lambda}{q}\right) \times\left(|\mathbf{p}-\mathbf{q}|(p+q+|\mathbf{p}-\mathbf{q}|)\frac{\delta_{\nu\tau}}{q}+\frac{p_\nu p_\tau}{p}+\frac{q_\nu p_\tau}{q}\right)\left(\delta_{\lambda\tau}-\frac{q_\lambda q_\tau}{q^2}\right). \quad (A38)$$

Its longitudinal part $\Pi_L^{(8)}(p) = p_\mu \Pi_{\mu\nu}^{(8)}(p) p_\nu / p^2$ is given by

$$\Pi_L^{(8)}(p) = \frac{2p}{\pi^2(1+c^2)}. \quad \text{(A39)}$$

Similarly, the longitudinal part $\Pi_L^{(9)}(p)$ is found to be

$$\Pi_L^{(9)}(p) = -\frac{4p}{\pi^2(1+c^2)}. \quad \text{(A40)}$$

The transverse part of the combined diagrams (8) and (9) is

$$\Pi_T^{(8)}(p) + \Pi_T^{(9)}(p) = -\frac{7p}{3\pi^2(1+c^2)}. \quad \text{(A41)}$$

Note that when diagrams (7), (8), and (9) are added the result is transverse,

$$\Pi_{\mu\nu}^{(7)}(p) + \Pi_{\mu\nu}^{(8)}(p) + \Pi_{\mu\nu}^{(9)}(p) = -\frac{4p}{3\pi^2(1+c^2)}\left(\delta_{\mu\nu} - \frac{p_\mu p_\nu}{p^2}\right). \quad \text{(A42)}$$

APPENDIX B: EVALUATION OF (A34) AND (A35)

In this appendix we derive identities (A34)–(A35), which are crucial for the derivation of the polarization tensors $\Pi_{\mu\nu}^{(4)}(p)$ and $\Pi_{\mu\nu}^{(8)}(p)$. We write the integral in terms of Lorentz invariant amplitudes

$$\int_k \frac{k_\mu}{k^2(k+p)^2(k+q)^2} = A p_\mu + B q_\mu. \quad \text{(B1)}$$

By contracting with p_μ and q_μ, we derive a system of linear equations for A and B:

$$A p^2 + B p\cdot q = I, \quad \text{(B2)}$$

$$A p\cdot q + B q^2 = J, \quad \text{(B3)}$$

with

$$I = \int_k \frac{k\cdot p}{k^2(k+p)^2(k+q)^2}, \quad \text{(B4)}$$

$$J = \int_k \frac{k\cdot q}{k^2(k+p)^2(k+q)^2}. \quad \text{(B5)}$$

Using $2k\cdot p = (k+p)^2 - p^2 - k^2$ in the integrand, we can easily calculate I and J with the help of (A1) and of formula (D1) (see Appendix D):

$$I = \frac{1}{16q|\mathbf{p}-\mathbf{q}|}(|\mathbf{p}-\mathbf{q}| - p - q), \quad \text{(B6)}$$

$$J = \frac{1}{16p|\mathbf{p}-\mathbf{q}|}(|\mathbf{p}-\mathbf{q}| - p - q). \quad \text{(B7)}$$

Solving the system of linear equations, we get

$$A = \frac{q^2 I - (p\cdot q)J}{p^2q^2 - (p\cdot q)^2}, \quad \text{(B8)}$$

$$B = \frac{p^2 J - (p\cdot q)I}{p^2q^2 - (p\cdot q)^2}. \quad \text{(B9)}$$

Substituting the expressions of I and J and simplifying, we get the results used in Appendix A.

Similarly, we write the other integral in terms of Lorentz invariant amplitudes:

$$\int_k \frac{k_\mu k_\nu}{k^2(k+p)^2(k+q)^2} = a\delta_{\mu\nu} + b p_\mu p_\nu + c(p_\mu q_\nu + q_\mu p_\nu) + d q_\mu q_\nu. \quad \text{(B10)}$$

By contracting with $\delta_{\mu\nu}$, p_μ, and q_μ, we obtain a system of linear equations for a, b, c, and d:

$$\begin{aligned} 3a + bp^2 + 2c(p\cdot q) + dq^2 &= K \\ aq^2 + b(p\cdot q)^2 + 2cq^2(p\cdot q) + dq^4 &= L \\ ap^2 + bp^4 + 2cp^2(p\cdot q) + d(p\cdot q)^2 &= M \\ a(p\cdot q) + bp^2(p\cdot q) + c(p^2q^2 + (p\cdot q)^2) + dq^2(p\cdot q) &= N, \end{aligned} \quad \text{(B11)}$$

where K, L, M, and N are basic integrals defined as follows:

$$\begin{aligned} K &= \int_k \frac{1}{(k+p)^2(k+q)^2} \\ L &= \int_k \frac{(k\cdot q)^2}{k^2(k+p)^2(k+q)^2} \\ M &= \int_k \frac{(k\cdot p)^2}{k^2(k+p)^2(k+q)^2} \\ N &= \int_k \frac{(k\cdot q)(k\cdot p)}{k^2(k+p)^2(k+q)^2}. \end{aligned} \quad \text{(B12)}$$

These basics integrals can be easily computed by using integral (A1) and (D1) after reducing the integrand when necessary with the formula $2k\cdot p = (k+p)^2 - p^2 - k^2$. Solving the system of linear equations, and simplifying the expressions, we get expressions for a, b, c, and d as given in Appendix A.

APPENDIX C: EVALUATION OF $G(1,1,1,1,1/2)$

In this appendix we compute $G(1,1,1,1,1/2)$. First, we simplify the integrand by multiplying and dividing by $2p\cdot q$ and using the following formula: $2p\cdot q=(k+p+q)^2-(k+p)^2-(k+q)^2+k^2$ in the numerator to reduce the number of propagators in the denominator to 4. This step gives, after some shifts in the variable of integration,

$$G(1,1,1,1,1/2)=\int_{k,q}\frac{1}{qk^2(k+p)^2(k+q)^2(k+p+q)^2}=2\int_{k,q}\frac{1}{q(p\cdot q)}\frac{1}{k^2(k+p)^2(k+q)^2}. \quad \text{(C1)}$$

Integrating over k first using formula (D1) (see Appendix D) gives

$$\begin{aligned}G(1,1,1,1,1/2)&=\frac{1}{4p}\int_q\frac{1}{q^2(p\cdot q)|\mathbf{p}-\mathbf{q}|}=\frac{1}{16\pi^2p^2}\int_0^\infty\frac{dq}{q}\int_{-1}^{1}\frac{du}{u\sqrt{p^2+q^2-2pqu}}\\&=-\frac{1}{8\pi^2p^2}\int_0^\infty\frac{dq}{q}\frac{1}{\sqrt{q^2+p^2}}\ln\left[\frac{\sqrt{q^2+p^2}+|q-p|}{\sqrt{q^2+p^2}+q+p}\right]\\&=-\frac{1}{8\pi^2p^3}\left[\frac{\pi^2}{12}+\frac{1}{2}\ln(1+\sqrt{2})\ln(2+2\sqrt{2})+di\log(1+\sqrt{2})+di\log(2+\sqrt{2})\right]. \quad \text{(C2)}\end{aligned}$$

APPENDIX D: EVALUATION OF THE SCALAR INTEGRAL (D1)

In this appendix we derive the following identity:

$$Z=\int_k\frac{1}{k^2(k+p)^2(k-q)^2}=\frac{1}{8pqs}, \quad \text{(D1)}$$

where $s=|\mathbf{p}+\mathbf{q}|$. Using a Feynman parametric representation, we transform this integral into

$$Z=\frac{1}{16\pi}\int_0^1dx\int_0^{1-x}dy\times\frac{1}{[x(1-x)q^2+y(1-y)p^2+2xy(\mathbf{p}\cdot\mathbf{q})]^{3/2}}. \quad \text{(D2)}$$

The integration over y is done first, and the expression obtained is greatly simplified with the help of Maple by using $2\mathbf{q}\cdot\mathbf{p}=(\mathbf{q}+\mathbf{p})^2-p^2-q^2$ beforehand. We obtain

$$Z=\frac{1}{8\pi}\frac{q+s}{qs(s^2-p^2)}\int_0^1dx\frac{1}{\sqrt{x(1-x)}}\frac{1}{x+u}, \quad \text{(D3)}$$

where $u=p^2/[(q+s)^2-p^2]$. Finally, the integration over x gives the desired result.

[1] R. Fazio and H. Van der Zant, Phys. Rep. **355**, 235 (2001).
[2] I. Osborne and R. Coontz, Science **319**, 1201 (2008); S. Sachdev, *Quantum Phase Transitions* (Cambridge University Press, Cambridge, England, 1999); S. L. Sondhi, S. M. Girvin, J. P. Carini, and D. Shahar, Rev. Mod. Phys. **69**, 315 (1997); M. Vojta, Rep. Prog. Phys. **66**, 2069 (2003).
[3] S. Sakhi, Physica (Amsterdam) **392A**, 6255 (2013); J. Phys. A **45**, 175301 (2012); **41**, 085003 (2008); S. Sakhi Europhys. Lett. **87**, 37006 (2009); **73**, 267 (2006); Phys. Rev. B **73**, 132505 (2006).
[4] M. C. Diamantini, P. Sodano, and C. A. Trugenberger, Nucl. Phys. **B474**, 641 (1996); **B448**, 505 (1995); Phys. Rev. Lett. **75**, 3517 (1995); Europhys. Lett. **83**, 21003 (2008).
[5] G. Parisi, J. Stat. Phys. **23**, 49 (1980).
[6] J. Zinn-Justin, *Quantum Field Theory and Critical Phenomena* (Clarendon, Oxford, 1989).
[7] H. E. Stanley, Phys. Rev. **176**, 718 (1968).
[8] S. K. Ma, *Modern Theory of Critical Phenomena* (Benjamin, New York, 1976).
[9] S. Coleman, R. Jakiw, and H. D. Politzer, Phys. Rev. D **10**, 2491 (1974).
[10] E. Brėzin and Zinn-Justin, Phys. Rev. B **14**, 3110 (1976).
[11] I. F. Herbut and Z. Tesanovic, Phys. Rev. Lett. **76**, 4588 (1996).
[12] M. Moshe and J. Zinn-Justin, Phys. Rep. **385**, 69 (2003).
[13] G. W. Semenoff, P. Sodano, and Y. S. Wu, Phys. Rev. Lett. **62**, 715 (1989).
[14] L. Halperin, T. C. Lubensky, and S. K. Ma, Phys. Rev. Lett. **32**, 292 (1974).
[15] M. Campostrini, A. Pelissetto, R Rossi, and E. Vicari, Nucl. Phys. **B459**, 207 (1996).
[16] Cha Min-Chul, P. A. Fisher Matthew, S. M. Girvin, and A. Peter Young, Phys. Rev. B **44**, 6883 (1991).